Supporting Information

3D MOF-derived Co-doped Cu_3P/NC octahedra embedded in 2D MXene nanosheets for efficient energy conversion

Mengmeng Zhang, Sining Yun*, Tianxiang Yang, Guangping Yang, Menglong Sun, Jiaoe Dang, Zhiguo Wang, Haijiang Yang, Shuangxi Yuan, Asim Arshad, and Ke Wang

Functional Materials Laboratory (FML), School of Materials Science and Engineering, Xi'an University of Architecture and Technology, Xi'an, Shaanxi, 710055, China

***Corresponding author**

E-mail: alexsyun1974@aliyun.com; yunsining@xauat.edu.cn

Including

Experimental section

Fig. S1 to S5

Table S1 to S3

Experimental section

Chemicals and materials

Cobalt nitrate hexahydrate ($Co(NO_3)_2·6H_2O$, Aladdin, 99%), copper nitrate trihydrate ($Cu(NO_3)_2·3H_2O$, Aladdin, 99%), 1,3,5-Trimesic acid (H_3BTC, Aladdin, 98%), Methanol (MeOH, Macklin, 99.5%), polyvinyl pyrrolidone (PVP, Aladdin, >99%), hydrofluoric acid (HF, Aladdin, AR, ⩾40%), sodium hypophosphite (NaH_2PO_2, Macklin, 99%) Lithium iodide (LiI, Alfa, 99.95%), iodine (I_2, Alfa, 99.5%), 1-butyl-3-methylimidazolium iodide (Aladdin, >99.0%), 4-tert butylpyridine (TBP, Macklin, >96.0%), guanidine thiocyanate (Macklin, 99.0%), lithium perchlorate ($LiClO_4$, Alfa, 99%), acetonitrile (Aladdin, 99.99%), chloroplatinic acid hexahydrate ($H_2PtCl_6·6H_2O$, Aladdin, Pt≥37.5%), and N719 dye (Solaronix SA) were commercially available and utilized without further purification. The MAX (Ti_3AlC_2) powders (400 mesh) were acquired from Foshan Xinxi Technology Co., Ltd., Guangdong, China.

Materials characterization

Scanning electron microscopy (SEM, ZEISS G500, Germany) and transmission electron microscopy (TEM, FEI TECNAI F20, America) were employed to analyze the micro-morphology of samples. X-ray diffraction (XRD, MDI D/Max 2200, America), Raman spectroscopy (LabRAM HR Evolution, Horiba, France) and N_2 adsorption-desorption measurements (ASAP 2460, America) were utilized to analyze the structural information of samples. The samples were analyzed for chemical bonding and elemental composition using X-ray photoelectron spectrometer (XPS, THERMO ESCALAB 250XI, America).

Electrode preparation

Preparation of HER electrode: The HER electrode was synthesized by mixing 10 mg of the electrocatalyst with a solution composed of 25 μL of Nafion and 975 μL of isopropanol. After 30 minutes of sonication, the catalyst suspension (75 μL) was uniformly dripped onto the nickel foam (NF) using a pipette gun and naturally dried. Prior to use, the NF was sliced into small pieces measuring 1 cm^2×2 cm^2 and soaked in a 2 M HCl solution for 30 min. Subsequently, the NF was rinsed until it reached a neutral pH and then dried at 60 °C. A Pt/C electrode with a weight

percentage of 20 wt% was employed in this work for preparation.

Preparation of counter electrode: The powders of MXene, Cu_3P/NC, Cu_3P/NC@MXene, and Co-Cu_3P/NC@MXene (120 mg each) were dispersed in 1.2 mL of isopropanol solution. A uniformly dispersed slurry was obtained by ball-milling for 4 h using ZrO_2 pearls as the milling medium. Subsequently, the catalyst slurry was sprayed onto a cleaned fluorine-doped tin oxide (FTO) glass substrate. The catalyst-covered FTO glass was subjected to annealing at 400 °C for 30 min under a nitrogen atmosphere to fabricate the intended counter electrode. The reference Pt electrode was fabricated through dip-coating FTO glass with an isopropanol solution of H_2PtCl_6, then annealing at 500 °C for 30 min.

Assembly of solar cells and symmetrical cells

The TiO_2 photoanode was annealed in air at 500 °C for 30 min, cooled to 120 °C and immersed in N719 dye solution for 24 h in dark. A sandwich-structured DSSC was formed by injecting I^-/I_3^- electrolyte between the counter electrode and the TiO_2 photoanode. The I^-/I_3^- electrolyte consisted of 0.06 M LiI, 0.03 M I_2, 0.6 M 1-butyl-3-methylimidazolium iodide, 0.5 M 4-tert-butylpyridine, and 0.1 M guanidine thiocyanate dissolved in acetonitrile, which is also the electrolyte used for *J-V* testing.[1, 2] In addition, two identical pair of counter electrodes and I^-/I_3^- electrolyte were combined to form the symmetrical cell.

Electrochemical and photovoltaic measurements

The cyclic voltammetry (CV) curves of the three-electrode system, consisting of Ag/Ag^+ (reference electrode, RE), Pt electrode (counter electrode, CE) and prepared electrode (working electrode, WE), were measured. The electrolytes for CV testing were prepared by dissolving I_2 (1 mM), LiI (10 mM), and $LiClO_4$ (0.1 M) in an acetonitrile solution. Tafel polarization and electrochemical impedance spectroscopy (EIS) tests were conducted on the prepared symmetrical dummy cell. EIS testing utilized an AC amplitude of 10 mV over frequencies ranging from 0.1 to 10^5 Hz. These measurement results were analyzed using Z-view software to create a model that represents an equivalent circuit. Photocurrent density-photovoltage (*J-V*) curves were obtained under 100 MW cm^{-2} illumination using a solar simulator (Xe arc lamp, EASISOLAR-50-3A,

CROWNTECH, INC., America) and a Keithley 2400 digital source meter. The stability of the prepared catalysts for IRR was assessed via a 50-turn CV testing.

Electrochemical measurements of HER

The electrochemical measurements for HER were conducted in a three-electrode system using a 1 M KOH solution saturated with nitrogen gas. In this system, the prepared MXene, Cu_3P/NC, Cu_3P/NC@MXene, and Co-Cu_3P/NC@MXene electrodes served as WE, with the graphite rod as CE, and an Hg/HgO electrode as RE. Linear scanning voltammetry (LSV) was conducted from -0.8 to -1.4 V. The reversible hydrogen electrode (RHE) was determined by applying the Nernst equation (Eq. 1).

$$E_{\mathrm{RHE}} = E_{\mathrm{Hg/HgO}} + 0.059 \times \mathrm{pH} + 0.098 \quad (1)$$

The Tafel slope is determined by analyzing the corresponding LSV curves using Eq. 2, where *a* represents a constant, *b* represents the Tafel slope, *j* signifies the current density, and η indicates the overpotential.

$$\eta = a + b\ log\ j \quad (2)$$

The EIS was carried out at an overpotential of 90 mV and within a frequency range spanning from 0.1 to 10^5 Hz. The electrochemical double-layer capacitance (C_{dl}) values were obtained by analyzing the CV curves acquired at various scan rates for all materials. The specific C_{dl} values were then derived by plotting Δj against the scan rate slope, where $\Delta j = |j_a - j_b|/2$. Finally, the electrochemically active surface area (ECSA) was computed using Eq. 3.

$$ECSA = \frac{C_{\mathrm{dl}}}{C_{\mathrm{s}}} \quad (3)$$

where C_s represents the specific capacitance, which was considered to be 40 μF cm^{-2}.[3]

The catalyst's stability for HER was evaluated by analyzing the LSV curve pre- and post-1000 cycles of CV test, as well as through a 30-hour chronopotentiometry (CP) test.

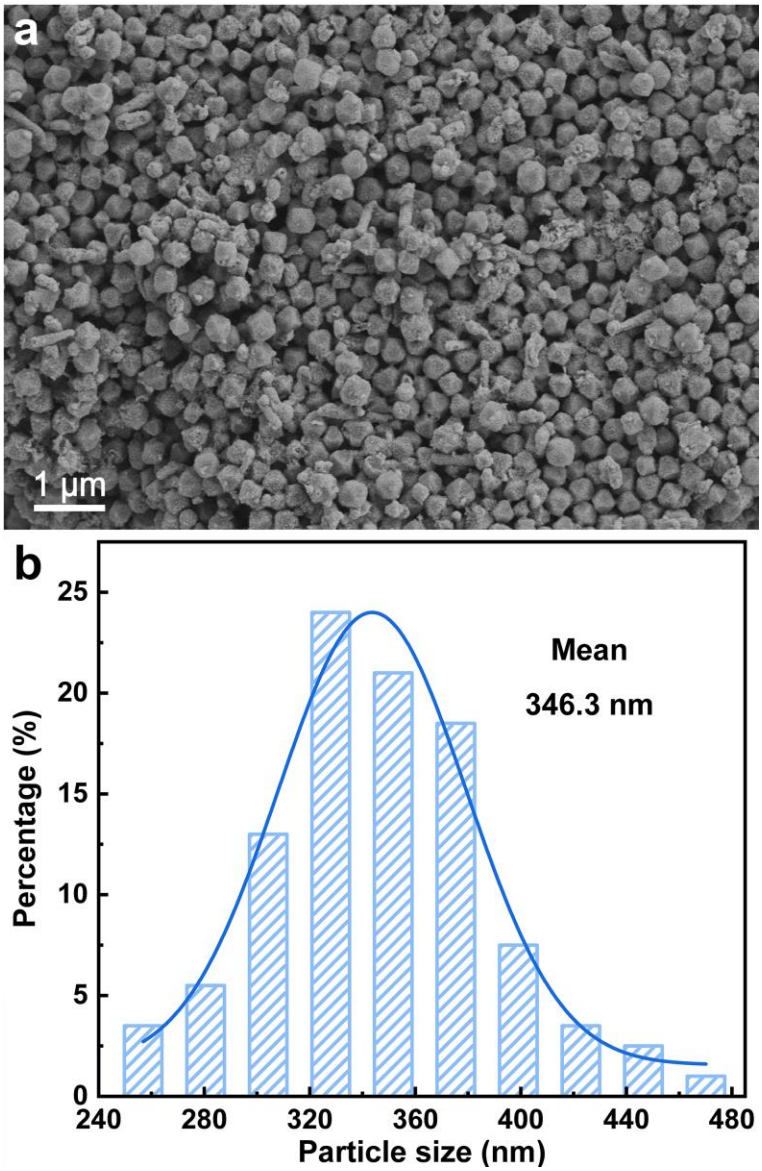

Fig. S1. (a) SEM images of Cu_3P/NC, (b)The illustration is the diameter distribution of Cu_3P/NC.

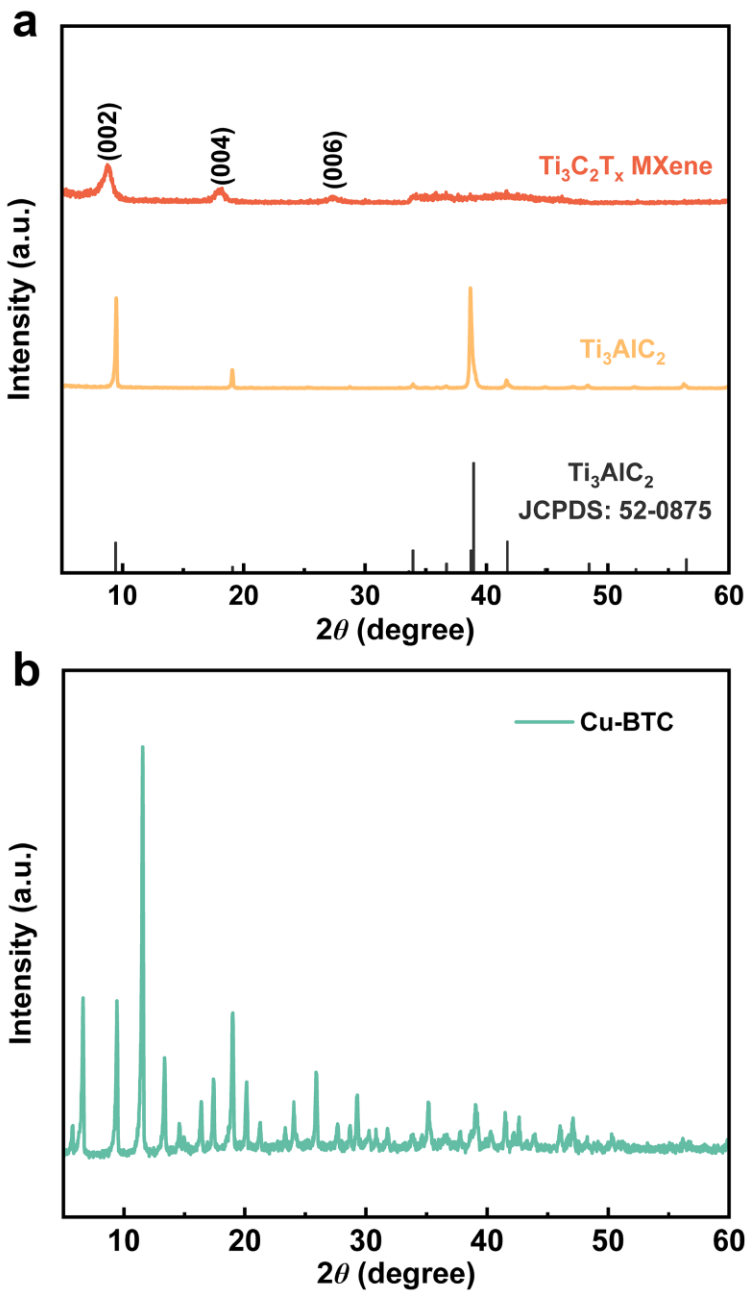

Fig. S2. XRD patterns of (a) Ti_3AlC_2 and $Ti_3C_2T_x$ MXene and (b) Cu-BTC.

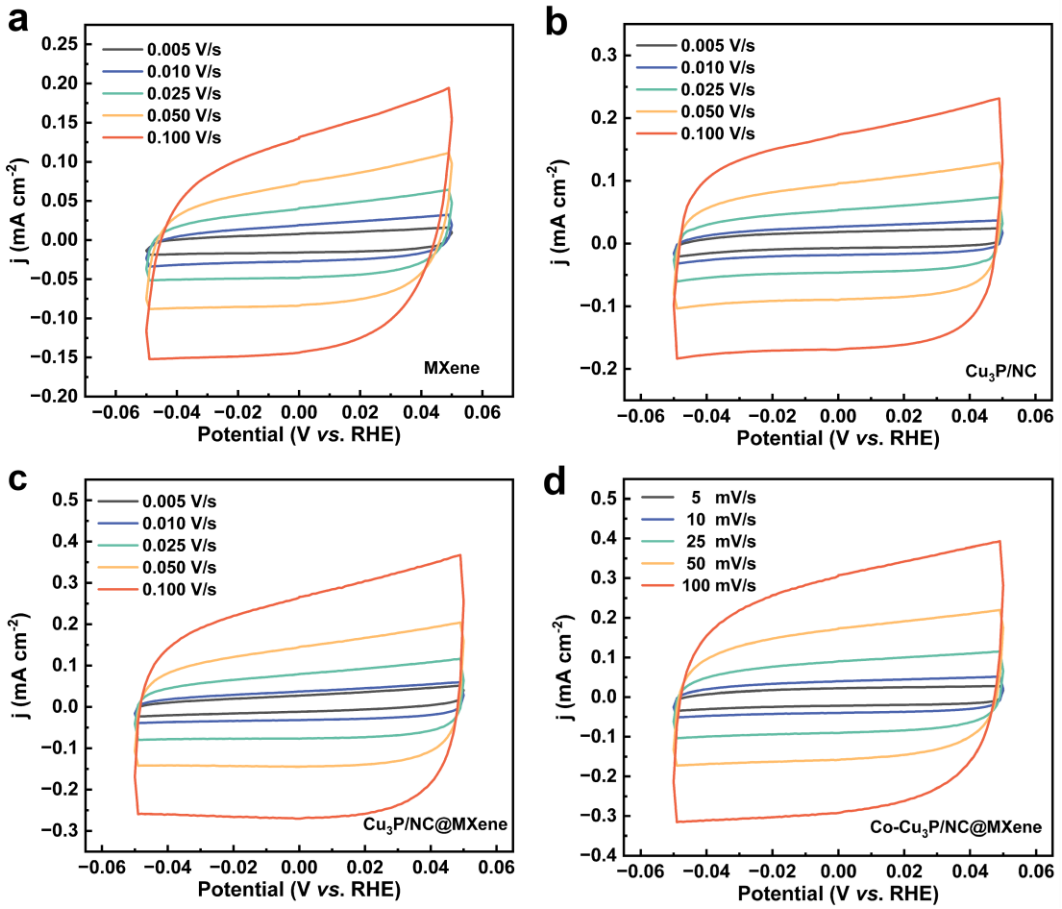

Fig. S3. CV curves of (a) MXene, (b) Cu_3P/NC, (c) Cu_3P/NC@MXene, (d) Co-Cu_3P/NC@MXene at different scan rates

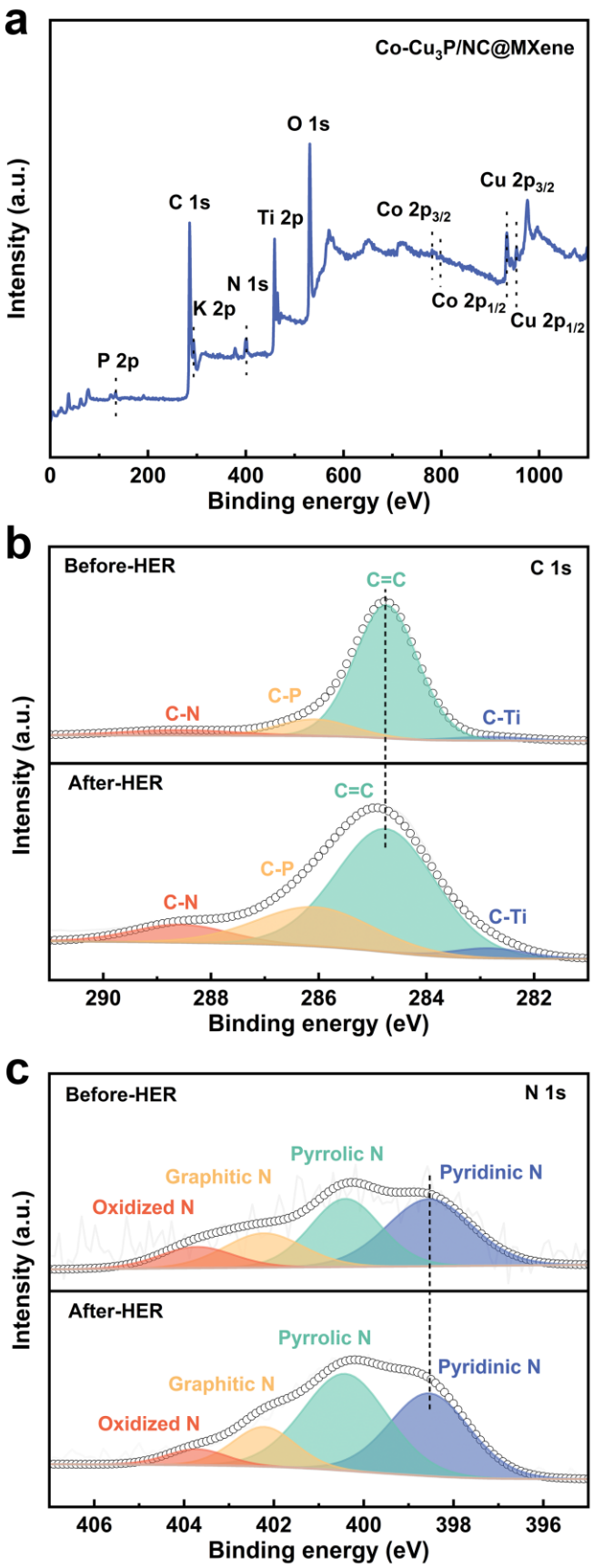

Fig. S4. (a) XPS survey spectra of Co-Cu_3P/NC@MXene after HER stability test. XPS spectrum of (b) C 1s and (c) N 1s for Co-Cu_3P/NC@MXene after HER stability test.

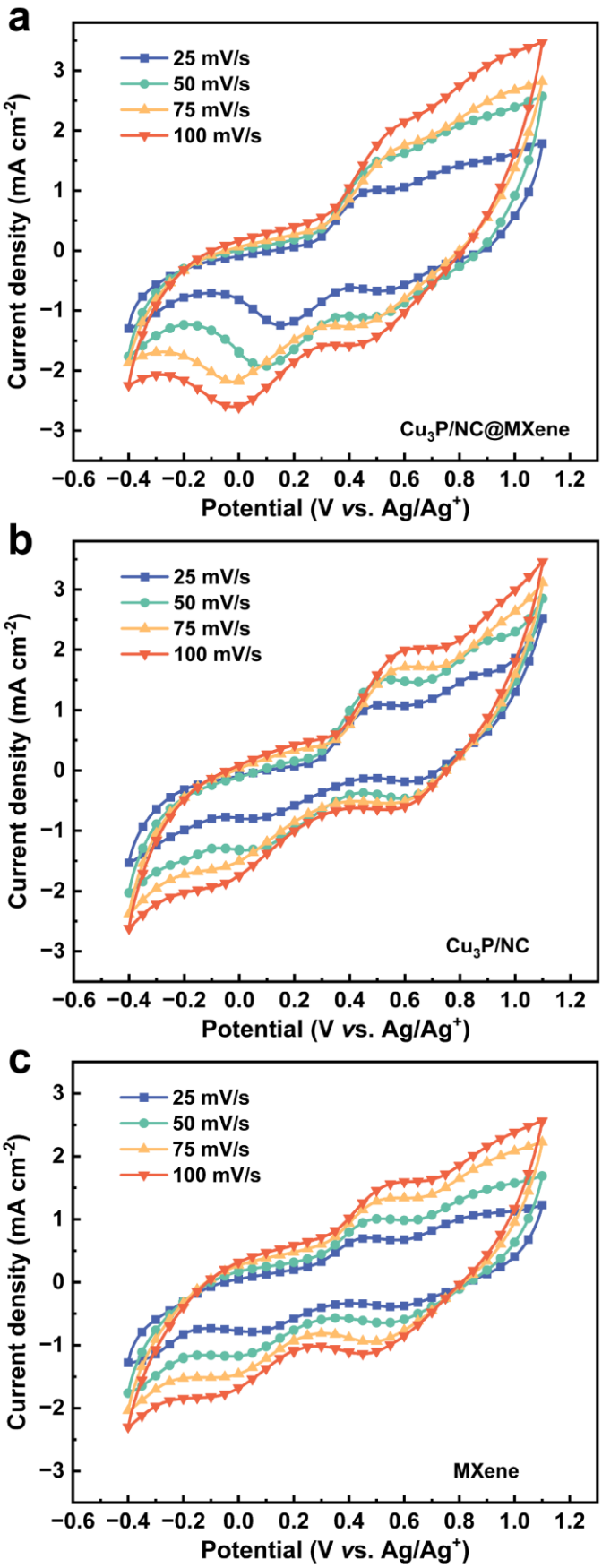

Fig. S5. CV curves of (a) Cu_3P/NC@MXene, (b) Cu_3P/NC, and (c) MXene under various scan rates.

Table S1. HER performance between Co-Cu_3P/NC@MXene and the previously reported non-noble metal electrocatalysts in 1 M KOH solution.

Electrocatalysts	Overpotential at 10 mA cm^{-2} (mV)	Tafel slope (mV dec^{-1})	Ref.
Ti_2NT_x@MOF-CoP	112	67.1	[4]
Cu_3P/CF	173	104	[5]
CoMoP	172	91	[6]
Fe-doped MOF CuCoSe	181	59	[7]
$CuCo_2S_4$	158	113	[8]
Ti_3C_2@mNiCoP	127	103	[9]
P-MoO_3 FCL MXene/NF	118	105	[10]
CoP/Mo_2CT_x	78	40	[11]
P-doped $CuCo_2O_4$	152	115.8	[12]
Mo-NiCo@MXene/NF	96	98.34	[13]
Co-Cu_3P/NC@MXene	**110**	**62**	**This work**

Table S2. Photovoltaic parameters of solar cells based on different counter electrodes.

Counter electrodes	J_{sc} (mA cm^{-2})	V_{oc} (V)	FF	PCE (%)
Pt	14.29±0.14	0.74±0.01	0.67±0.01	7.16±0.12
MXene	12.37±0.24	0.76±0.02	0.67±0.02	6.26±0.24
Cu_3P/NC	13.60±0.10	0.73±0.01	0.67±0.01	6.67±0.08
Cu_3P/NC@MXene	14.47±0.02	0.76±0.01	0.72±0.01	7.95±0.11
Co-Cu_3P/NC@MXene	15.14±0.02	0.76±0.01	0.72±0.01	8.20±0.05

Table S3. Photovoltaic parameters of solar cells with different CEs in I_3^-/I^- electrolyte and N719 dye.

Counter electrodes	J_{sc} (mA cm^{-2})	V_{oc} (V)	FF	PCE (%)	Ref.
NiS@$CoNi_2S_4$	15.73	0.77	0.65	7.96	[14]
$CoNiTe_2$/SNTC	16.71	0.76	0.64	8.11	[15]
$Cu_3Mo_2O_9$/3D-AWC	15.71	0.74	0.63	7.33	[16]
$CuTa_{10}O_{26}$/SC	15.19	0.68	0.63	6.53	[17]
$CuCo_2O_4$@RGO	12.11	0.79	0.64	6.11	[18]
$Ni_{12}P_5$/C	13.88	0.76	0.75	7.94	[19]
rGO-NCS	16.40	0.75	0.66	8.15	[20]
CESM-$CuInS_2$	12.48	0.78	0.60	5.79	[21]
Cu/P25-Cu/Pt	17.91	0.72	0.58	7.62	[22]
CoP_3	13.91	0.82	0.60	6.84	[23]
Co-Cu_3P/NC@MXene	**15.18**	**0.76**	**0.71**	**8.18**	**This work**

Reference

1. J. Dang, S. Yun, Y. Zhang, J. Yang, Z. Liu, C. Dang, Y. Wang and Y. Deng, *Chem. Eng. J.*, 2022, **449**, 137854.
2. M. Sun, S. Yun, J. Shi, Y. Zhang, A. Arshad, J. Dang, L. Zhang, X. Wang and Z. Liu, *Small*, 2021, **17**, 2102300.
3. C. C. L. McCrory, S. Jung, J. C. Peters and T. F. Jaramillo, *J. Am. Chem. Soc.*, 2013, **135**, 16977-16987.
4. H. Zong, R. Qi, K. Yu and Z. Zhu, *Electrochim. Acta*, 2021, **393**, 139068.
5. J. Chen, X. Li, B. Ma, X. Zhao and Y. Chen, *Nano Res.*, 2021, **15**, 2935-2942.
6. X. Huang, X. Xu, X. Luan and D. Cheng, *Nano Energy*, 2020, **68**, 104332.
7. S.-H. Chae, A. Muthurasu, T. Kim, J. S. Kim, M.-S. Khil, M. Lee, H. Kim, J. Y. Lee and H. Y. Kim, *Appl. Catal. B: Environ.*, 2021, **293**, 120209.
8. C. Zequine, S. Bhoyate, F. Wang, X. Li, K. Siam, P. K. Kahol and R. K. Gupta, *J. Alloys Compd.*, 2019, **784**, 1-7.
9. Q. Yue, J. Sun, S. Chen, Y. Zhou, H. Li, Y. Chen, R. Zhang, G. Wei and Y. Kang, *ACS Appl. Mater. Interfaces*, 2020, **12**, 18570-18577.
10. M. Li, R. Sun, Y. Li, J. Jiang, W. Xu, H. Cong and S. Han, *Chem. Eng. J.*, 2022, **431**, 133941.
11. S. Liu, Z. Lin, R. Wan, Y. Liu, Z. Liu, S. Zhang, X. Zhang, Z. Tang, X. Lu and Y. Tian, *J. Mater. Chem. A*, 2021, **9**, 21259-21269.
12. S. Tan, Y. Ji, F. Ren, F. Chen and W. Ouyang, *Int. J. Hydrog. Energy*, 2022, **47**, 9248-9260.
13. J. Jiang, R. Sun, X. Huang, W. Xu, S. Zhou, Y. Wei, S. Han and Y. Li, *Compos. B. Eng.*, 2023, **263**, 110834.
14. J. Dang, S. Yun, Y. Zhang, G. Yang, J. Yang, D. Qiao and T. Yang, *J. Colloid Interface Sci.*, 2023, **630**, 91-105.
15. Y. Deng, S. Yun, J. Dang, Y. Zhang, C. Dang, Y. Wang, Z. Liu and Z. Gao, *J. Colloid Interface Sci.*, 2022, **624**, 650-669.
16. F. Han, S. Yun, J. Shi, Y. Zhang, Y. Si, C. Wang, N. Zafar, J. Li and X. Qiao, *Appl. Catal. B: Environ.*, 2020, **273**, 119004.
17. S. Yun, X. Zhou, Y. Zhang, C. Wang and Y. Hou, *Electrochim. Acta*, 2019, **309**, 371-381.
18. K. Xiong, W. Nie, P. Yu, L. Zhu and X. Xiao, *Materials Letters*, 2017, **204**, 69-72.
19. M. Chen, L.-L. Shao, Z.-Y. Yuan, Q.-S. Jing, K.-J. Huang, Z.-Y. Huang, X.-H. Zhao and G.-D. Zou, *ACS Appl. Mater. Interfaces*, 2017, **9**, 17949-17960.
20. K. S. Anuratha, M. Ramaprakash, S. K. Panda and S. Mohan, *Ceram. Int.*, 2017, **43**, 10174-10182.
21. L. Wang, J. He, M. Zhou, S. Zhao, Q. Wang and B. Ding, *J. Power Sources*, 2016, **315**, 79-85.
22. Y. Jiang, Y. Yang, L. Qiang, T. Ye, L. Li, T. Su and R. Fan, *J. Power Sources*, 2016, **327**, 465-473.
23. X. Gao, G. Yue, R. Cheng, T. Wu, L. Fan, Y. Gao and F. Tan, *Sol. Energy*, 2020, **208**, 289-295.